Modern Health Science; Vol. 8, No. 2; 2025
ISSN 2576-7291 E-ISSN 2576-7305
https://doi.org/10.30560/mhs.v8n2p35

# Synthesis, Crystal Structure, and Cytotoxicity Analysis of Dichloro-(2,2′:6′,2″-Terpyridine)-Copper(II)

Nan Jin[1], Lang Zhang[1] & Xiu-Ying Qin[1]

[1] College of Pharmacy, Guilin Medical University, China

Correspondence: Xiu-Ying Qin, College of Pharmacy, Guilin Medical University, Guangxi Guilin, 541004, China. E-mail: xyqin6688@163.com

Received: April 16, 2025; Accepted: April 28, 2025; Published: April 30, 2025

**Abstract**

Malignant tumors, recognized as one of the most threatening diseases of the 20th century, continue to exhibit a rising incidence trend in the 21st century. Against this backdrop, metal complexes have attracted considerable attention due to their unique antitumor activities. In this study, we unexpectedly obtained a copper-based complex coordinated with 2,2':6',2"-Terpyridine and chloride anion ligands, and characterized its crystal structure using X-ray single-crystal diffraction technique. The cytotoxic effects of this metal complex against various tumor cell lines were evaluated through MTT assays, and the findings provide significant theoretical and practical foundations for developing novel anticancer drugs.

**Keywords:** Copper (II) complex, Crystal structure, Cytotoxicity, Cancer cells

## 1. Introduction

As one of the essential trace elements for the human body, copper is second only to iron in its biological importance and plays a crucial role in the process of cellular metabolism [1]. Copper is abundant in resources and low in cost, and it has the characteristic of multiple valence states ($Cu^0/Cu^+/Cu^{2+}$), enabling it to form coordination bonds with heteroatoms such as chlorine, nitrogen, and oxygen, and to construct stable complexes with diverse structures [2-3]. In the field of anti-tumor drug research and development, copper complexes are regarded as highly promising alternative candidate drugs because they have lower toxicity and higher safety compared with platinum-based drugs, and also possess multiple pharmacological activities such as antibacterial, anti-tuberculosis, and anti-malaria activities [4]. For example, the copper (II) complex of salicylate phenanthroline is a new type of drug for the treatment of triple-negative breast cancer, with broad prospects and worthy of further research [5]. In addition, the previous research of our research group has confirmed that copper (II) complexes designed based on different ligands have shown remarkable effects in various areas of biological activity, including inhibiting the proliferation of ovarian cancer, breast cancer, and triple-negative breast cancer cells, and also having synergistic effects such as anti-inflammatory, anti-apoptotic, and anti-angiogenic activities [6-9]. With the advantages of their unique electronic structure characteristics [10], high-efficiency catalytic ability, and biological activities [11], copper complexes have been widely applied in many fields, such as materials science, biomedicine, and drug research and development, and have demonstrated extremely broad application prospects [12].

Halogens (especially chlorine) play a crucial role in drug design [13]. At the molecular level, as a monodentate ligand, chlorine can form stable coordination bonds with metal centers such as platinum and ruthenium [14]. This coordination not only determines the spatial configuration and charge distribution of the complex (for example, the cis-configuration of Cl coordination in cisplatin is a key structural feature for its anti-tumor activity), but also affects the drug activity by regulating the hydrolysis rate ($Cl^-$ is easily replaced by water molecules to form active species). In terms of pharmacodynamics, the hydrolysis products of chlorine ligands can regulate the anion balance within tumor cells [15-16], participate in the generation of reactive oxygen species (ROS) to induce oxidative stress, and promote apoptosis by affecting the mitochondrial membrane potential. These findings provide important theoretical bases for the design of new metal anti-tumor drugs.

2,2':6',2"-Terpyridine, as an important class of polydentate nitrogen-containing ligands, has unique advantages in drug design. Its three pyridine nitrogen atoms can form a stable tridentate chelating structure with metal centers such as Cu (II) and Co (II) [17-19]. This rigid planar configuration not only enhances the steric stability of the complex, but also can specifically bind to DNA bases through π-π stacking interactions, significantly improving the targeting ability [20]. These findings provide important ideas for the development of new metal anti-tumor

drugs. In this paper, 5-bromo-2-hydroxy-3-methoxybenzaldehyde, potassium hydroxide, L-tyrosine, 2,2':6',2''-terpyridine and copper chloride were used as raw materials and synthesized by the solution method in anhydrous methanol. Its synthetic route is shown in Scheme 1.

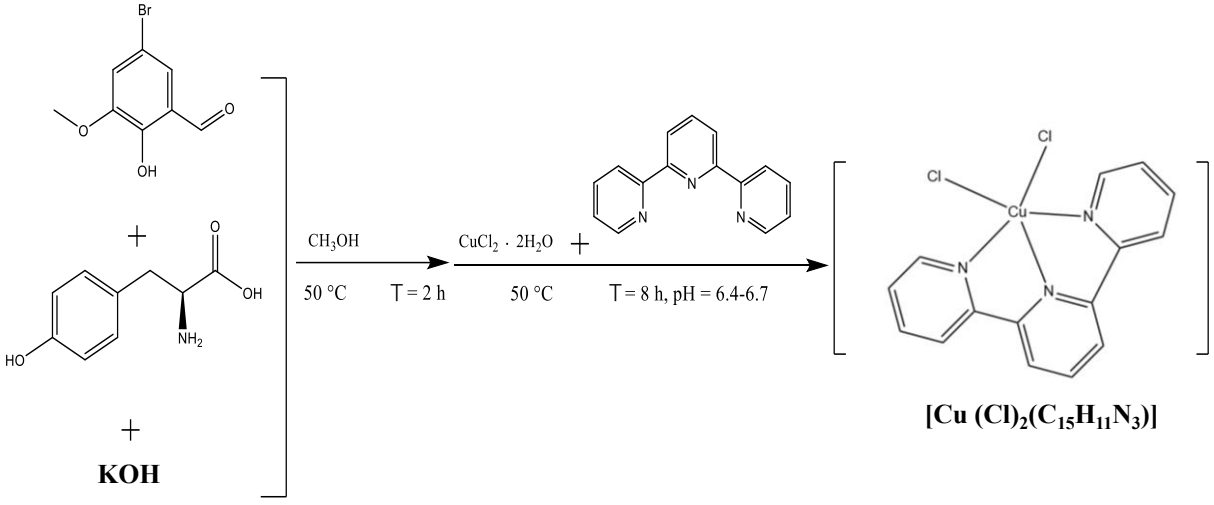


Scheme 1. Synthesis route of (I).

## 2. Materials and Methods

### *2.1 Experimental Reagents and Instruments*

**Materials.** Unless otherwise specified, all materials and solvents were purchased commercially. Ultrapure Milli-Q water was used in all experiments. 5-Bromo-2-hydroxy-3-methoxybenzaldehyde (A.R.), L-tyrosine (A.R.), copper chloride dihydrate (A.R.), 2,2':6',2''-terpyridine (A.R.) were purchased from Aladdin. Anhydrous methanol (A.R.) was purchased from Xilong Technology Co., LTD. Potassium hydroxide (R.G.) was purchased from Adamas. MTT, penicillin / streptomycin, dimethyl sulfoxide (DMSO) and bovine serum albumin (BSA) were purchased from Solarbio (Beijing, China). dimethyl sulfoxide-d6 (DMSO-d6) were purchased from Innochem (Beijing, China). Dulbecco's modified eagle medium (DMEM, Gibco), Fetal bovine serum (FBS, GEMINI), pancreatic enzyme (Gibco), cell culture plates (Corning) were used. Cell culture: the complete medium was prepared by adding fetal bovine serum (10%), penicillin (100 μg/mL) and streptomycin (100 μg/mL) to DMEM medium. The cells were cultured in a humidified incubator with 37℃, 5% $CO_2$ and 95% air, and the culture medium was changed three times a week.

**Instruments.** Beaker, Round-bottom flask, Allihn condenser, Water bath. The crystal structures were determined by a four-circle CCD diffractometer (XtaLAB Synergy, Dualflex, HyPix).

### *2.2 Synthesis of (I)*

5-bromo-2-hydroxy-3-methoxybenzaldehyde (0.1mmol, 0.0240g) was dissolved in 7mL absolute methanol, potassium hydroxide (0.3mmol, 0.0180g) and L-tyrosine (0.1mmol, 0.0192g) were dissolved in 9mL absolute methanol, and the two solutions were mixed. The reaction was heated at 50℃, stirred and reflow for 2 hours to obtain a yellow solution. Then, 2mL of methanol solution containing 2,2′:6′,2″-Terpyridine (0.1mmol, 0.0234g) and 2 mL of methanol solution containing copper chloride (0.1mmol, 0.0189g) were added to the aforesaid yellow solution, and the pH value of the mixture was adjusted to between 6.4 and 6.7, and the reaction solution turned from yellow to green. The reaction was continued at 50 °C for 8h with stirring and reflux. At the end of the reaction, the reaction solution was cooled, filtered to remove the brown powder, and the bright green solution was allowed to evaporate slowly at room temperature, and green needle crystals (5.9 mg) were obtained after several days.

### *2.3 X-Ray Crystallography*

A green single crystal of (I) of appropriate size was selected for measurement. The crystallographic data of (I) were collected on a four-circle diffractometer (Type: XtaLAB Synergy, Dualflex, HyPix) equipped with X-ray mirror-monochromatized Cu K\a radiation (λ = 1.54184Å) in the omega scan mode at temperature 296.21(10) K. For computing data collection, cell refinement, and data reduction were performed with CrysAlisPro 1.171.43.95a (Rigaku OD, 2023). Using Olex2 1.5 application program (Dolomanov et al., (2009) [21], the SHELXT 2018/2 (Sheldrick, 2018) program was used to solve the structure and the SHELXL 2018/3 (Sheldrick, 2015) program

[22] was used to refine the crystal structure. All atoms were refined by anisotropic displacement parameters. All H atoms bonded to C atoms were calculated hydrogens, with C–H = 0.9300 Å for aromatic [Uiso(H) = 1.2 Ueq(C)]. The CIF file on the crystal data was deposited in the Cambridge Crystallographic Data Center.

*2.4 MTT Cell Cytotoxicity Assay*

All cell lines used in this study were purchased from Shanghai Aolu Biotechnology Co., Ltd. Among them, cancer cell lines (MCF-7, MDA-MB-231, SKOV3, HepG2, and MGC-803) and non-cancerous human umbilical vein endothelial cells (HUVECs) were cultured in high-glucose DMEM medium (containing 10% fetal bovine serum and 1% penicillin-streptomycin double-antibiotic solution); human renal tubular epithelial cell line (HK-2) was cultured in a specific medium. All cells were routinely cultured in an incubator at a constant temperature of 37°C, with a $CO_2$ concentration of 5% and a relative humidity of 95%. During the experiment, different concentrations of the metal complex (I) was co-cultured with each cell line for 48 hours, and then the MTT method was used to detect its cytotoxic effect. The cell proliferation inhibition rate was calculated according to the following formula: (Absorbance value of the control group - Absorbance value of the experimental group) / (Absorbance value of the control group - Absorbance value of the blank control group) × 100%. The experimental data were analyzed by non-linear regression using SPSS statistical software to calculate the half maximal inhibitory concentration ($IC_{50}$). Furthermore, GraphPad Prism software was used for data visualization, drawing bar charts of the concentration-dependent inhibition rate, and analyzing the statistical differences in the inhibitory effects among different groups.

## 3. Results

*3.1 The Crystal Structure of (I)*

The crystallographic data suggest that the structure of (I) is crystallized in a monoclinic crystal system with a space group $P2_1/c$ and with the cell parameters: $a$ = 10.6894(3) Å, $b$ = 8.2548(2)Å, $c$ = 16.0871(4) Å, $\alpha = \gamma = 90°$, $\beta$ = 94.617(2) °, $V$ = 1414.90(6) Å$^3$, $Z$ = 4, $Dc$ = 1.726 g/cm$^3$, $F$ (000) = 740, $\mu$ = 5.605 mm$^{-1}$, $S$ = 1.070, $R_1$= 0.0333, $\omega R_2$ = 0.0933, $Mr$ = 367.71, Formula = $C_{15}H_{11}Cl_2CuN_3$. Other crystal data were given in Table 1, and the coordinated bond lengths and angles were listed in Table 2, and hydrogen bonds were listed in Table 3. All crystallographic data were deposited in the Cambridge Crystallographic Data Center (CCDC Number: 2343630; deposit@ccdc.cam.ac.uk). The crystal structure diagram of (I) is shown in Figure 1. (I) consists of a neutral ligand (2,2′:6′,2″-Terpyridine) and two chloride anion ligands and a divalent copper ion, [Cu $(Cl)_2(C_{15}H_{11}N_3)$], namely dichloro-(2,2′:6′,2″-Terpyridine)-copper(II), where $C_{15}H_{11}N_3$ =2,2′:6′,2″-Terpyridine. In the structure of **(I)**, Cu1 is coordinated with three coordination nitrogen atoms (N1, N2, and N3) from 2,2′:6′,2″-Terpyridine ligand and two chlorine atoms (Cl1 and Cl2) from chloride anion ligands to form a five-coordinated tetragonal pyramid geometry （$\tau$ = (157.32-156.20)/60 = 0.019, $\tau$ is very close to zero). In the tetragonal pyramid geometry, the sum of the bond angles < N3Cu1Cl2 =97.35(9) °, < N2Cu1N3 = 78.71(13) °, < N2Cu1N1 = 79.27(13) °, < N1Cu1Cl2 = 99.48(9) ° is 354.81° (see: Table 2), indicating that the Cu1 atom deviates from plane N1N2N3Cl2. Cl1 is the vertex of a tetragonal pyramid geometry. The bond lengths of coordination bond Cu-Cl are larger than those of coordination bond Cu-N, and the bond length of coordination bond Cu1-Cl2 is the largest, as shown in Table 2. There are atypical hydrogen bonds (C-H ... Cl) and π … π stacking effects between molecules (see: Figure 2). It is these intermolecular forces that stabilize the crystal structure of (I).

Table 1. Crystal data and structure refinement parameters for (I)

| **parameters** | **(I)** | **parameters** | **(I)** |
|---|---|---|---|
| Formula moiety | $C_{15}H_{11}Cl_2CuN_3$ | $D_c$ (g cm$^{-3}$) | 1.726 |
| Structural formula | [Cu $(Cl)_2(C_{15}H_{11}N_3)$] | θ range (°) | 6.0160 ~51.5760 |
| Formula weight | 367.71 | Abs. coefficient (mm$^{-1}$) | 5.605 |
| Crystal system | Monoclinic | F (000) | 740 |
| Space group | $P2_1/c$ | | -10 ≤ h ≤ 6 |
| Temperature (K) | 296.21(10) | Limiting indices | -8 ≤ k ≤ 7 |
| Radiation type | Cu K\a | | -14 ≤ l ≤ 15 |
| Wavelength (Å) | 1.54184 | Measured refls | 1310 |
| *a(Å)* | 10.6894(3) | Independent refls | 1211 |
| *b(Å)* | 8.2548(2) | $R_{int}$ | 0.0254 |
| *c(Å)* | 16.0871(4) | Goodness | 1.07 |
| *α(°)* | 90 | H-atom treatment | constr |
| *β(°)* | 94.617(2) | Nref / Npar / Nres | 1310/190/0 |
| *γ(°)* | 90 | $R_1$/w$R_1$ | 0.0333 / 0.0916 |

| | | | |
|---|---|---|---|
| *V*(Å$^3$) | 1414.90(6) | $R_2$/w$R_2$ | 0.0351/ 0.0933 |
| *Z* | 4 | Shift max / mean | 0.001 / 0.000 |

Table 2. Selected bond distances (Å) and angles (°) for (I).

| **Bond** | **Dist. (Å)** | **Bond** | **Dist. (Å)** |
|---|---|---|---|
| Cu1 — Cl1 | 2.4712(11) | Cu1 — Cl2 | 2.2490(10) |
| Cu1 — N2 | 1.962(3) | Cu1 —N3 | 2.055(3) |
| Cu1 — N1 | 2.061(3) | | |
| **Angle** | **(°)** | **Angle** | **(°)** |
| N2 — Cu1— Cl1 | 98.22(9) | N2 — Cu1— Cl2 | 157.32(10) |
| N2 — Cu1— N3 | 78.71(13) | N2 — Cu1— N1 | 79.27(13) |
| N3 — Cu1— Cl1 | 99.26(9) | N3 — Cu1— Cl2 | 97.35(9) |
| N3 — Cu1— N1 | 156.20(13) | N1 — Cu1— Cl1 | 92.71(9) |
| N1 — Cu1— Cl2 | 99.48(9) | | |

Table 3. Hydrogen bond lengths (Å), angles (°) for (I)

| ***D*—H••• *A*** | ***D*—H** | **H ••• *A*** | ***D* ••• *A*** | **<*D*H*A*** |
|---|---|---|---|---|
| C7—H7••• *Cl2*$^{\#1}$ | 0.93 | 2.95 | 3.668(4) | 134.8 |
| C1—H1 ••• *Cl2* | 0.93 | 2.96 | 3.484(5) | 117.3 |
| C12—H12••• *Cl1*$^{\#2}$ | 0.93 | 2.62 | 3.488(4) | 155.8 |
| C15—H15••• *Cl2* | 0.93 | 2.89 | 3.413(4) | 116.9 |
| C14—H14 ••• *Cl1*$^{\#3}$ | 0.93 | 2.77 | 3.457(4) | 131.5 |

Symmetry codes: (#1) +X, 0.5-Y, -0.5+Z; (#2) 2-X, 1-Y, 1-Z; (#3) 2-X, 0.5+Y, 1.5-Z.

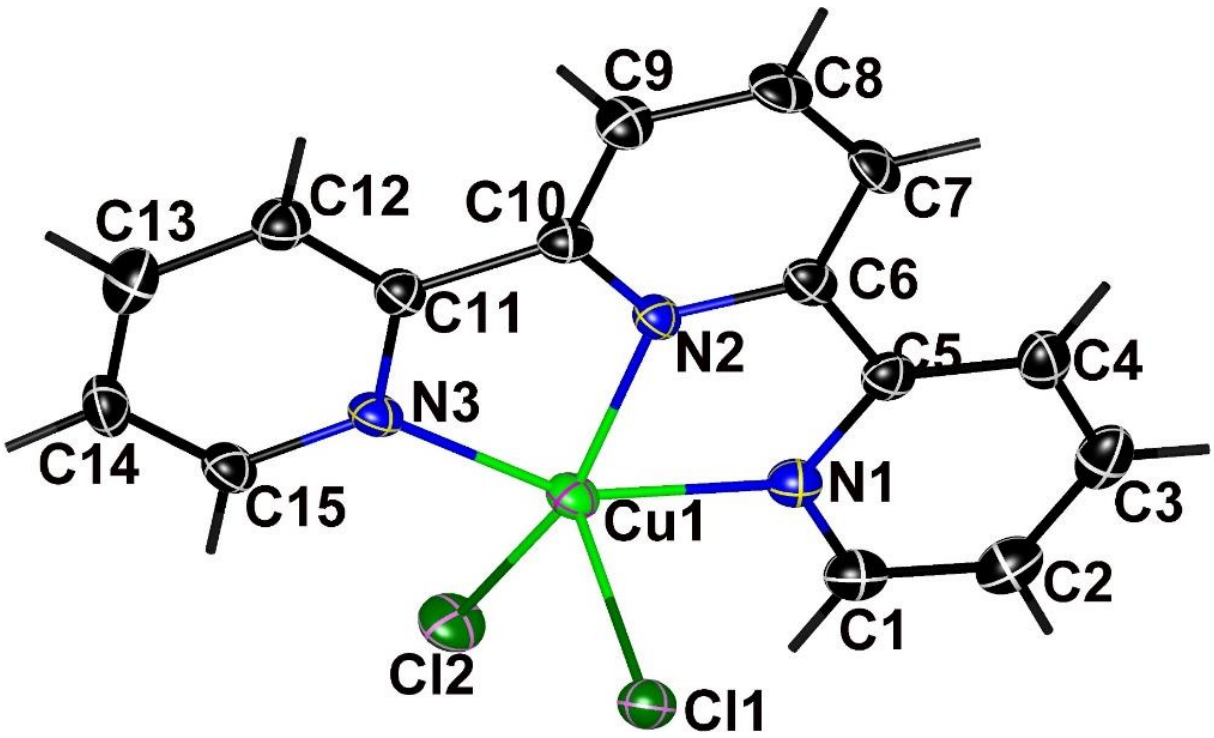


Figure 1. The crystal structure view of (I) with atom labels and 50% probability displacement ellipsoids

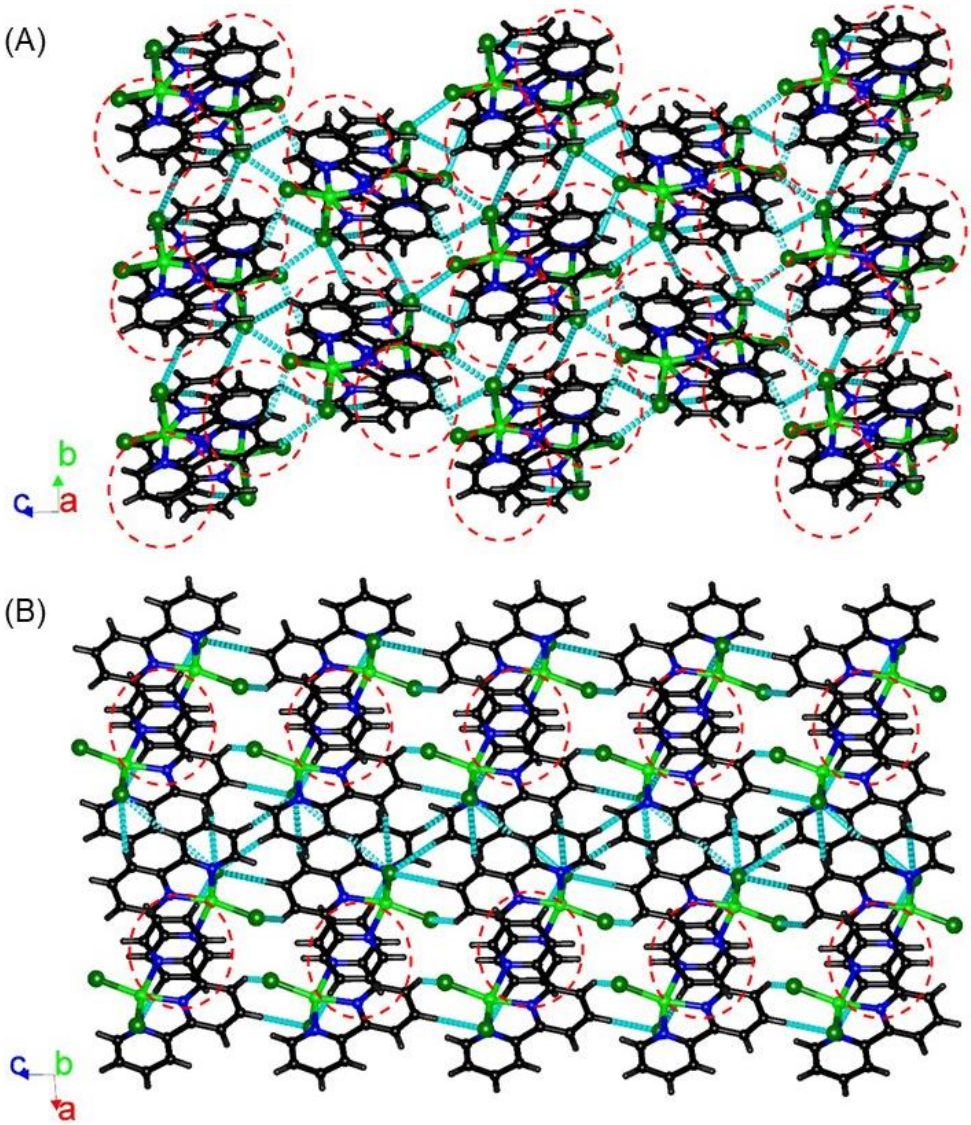


Figure 2. The packings of (I), viewed down the a axis(A) and down the b axis(B), showing a two-dimensional network structure through the atypical hydrogen bond C—H ...Cl (dashed lines). π … π stackings are present in the area of the red dashed lines

*3.2 MTT Cytotoxicity Experiment*

The cytotoxicity of (I) against five kinds of cancer cells (MCF-7, MDA-MB-231, SKOV3, HepG2, MGC-803) and two kinds of non-cancerous human umbilical vein endothelial cells (HUVECs) and human renal tubular epithelial cells (HK-2) was detected by the MTT method. The experimental results are shown in Table 4 and Figure 3.The experimental results show that after these cells were incubated with different concentrations of (I) for 48 hours, the cytotoxicity to all the tested cells was as follows: the $IC_{50}$ values for MCF-7, MDA-MB-231, SKOV3, and HepG2 cells were (24.525 ± 1.16) μM, (58.59 ± 1.54) μM, (41.63 ± 1.98) μM, and (52.88 ± 3.86) μM respectively, indicating moderate cytotoxicity. The $IC_{50}$ value for MGC-803 cells was (166.81 ± 3.19) μM, showing weak cytotoxicity. The cytotoxicity to non-cancerous HUVECs cells and HK-2 cells was even weaker, with $IC_{50}$ values of (273.98 ± 8.24) μM and (292.78 ± 18.50) μM respectively. When the concentration of (I) was 160 μM, the inhibition rates for MCF-7, MDA-MB-231, SKOV3, HepG2, MGC-803, HUVECs, and HK-2 cells were (86.59 ± 0.46) %, (59.91 ± 1.14) %, (74.28 ± 0.68) %, (61.28 ± 1.82) %, (49.38 ± 0.64) %, (42.13 ± 2.11) %, and (42.66 ± 0.03) %, respectively. These data indicate that the toxicity of (I) to the tested cancer cells is greater than that to non-cancer cells, reflecting good selective cytotoxicity to cancer cells. Among these tested cells, (I) has the best inhibitory effect on the growth of MCF-7 cells.

Table 4. Shows the $IC_{50}$ values of (I) against various tumor cells after 48 hours of treatment

| | $IC_{50}$ (μM) | | | |
|---|---|---|---|---|
| **(I)** | MCF-7 | MDA-MB-231 | SKOV3 | Hepg2 |
| | 25.53 ± 1.16 | 58.59 ± 1.54 | 41.63 ± 1.98 | 52.88 ± 3.86 |
| | MGC-803 | HUVECs | HK-2 | |
| | 166.81.41± 3.19 | 273.98 ± 8.24 | 292.78.35± 18.49 | |

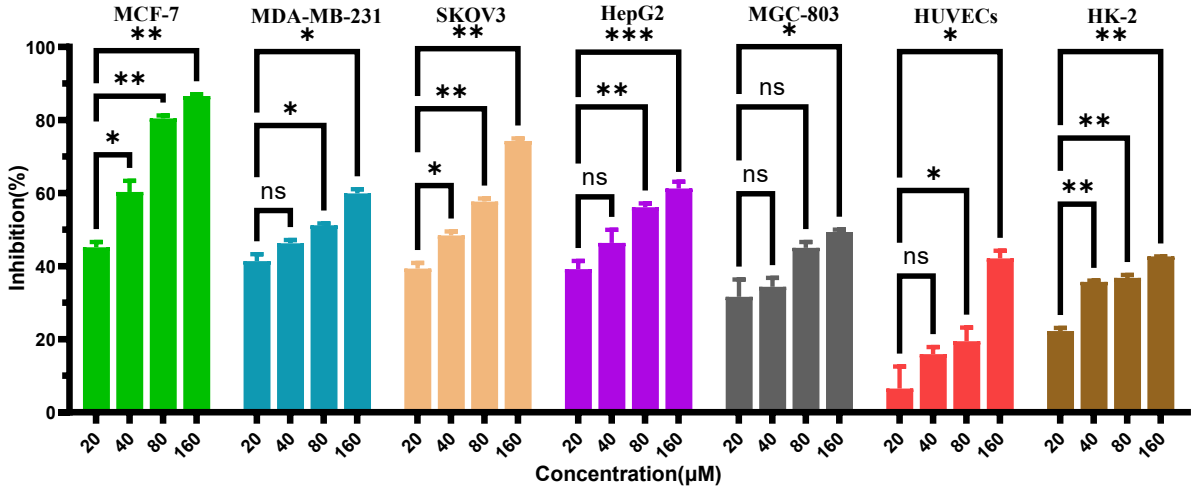


Figure 3. Explores the influence of (I) at different concentrations on the inhibition rates of various cells. For each cell type, the statistical significance differences between the treatment group and the control group were determined respectively. * $p < 0.05$; ** $p < 0.01$; *** $p < 0.001$; **** $p < 0.0001$

## 4. Conclusions

In this study, using 5-bromo-2-hydroxy-3-methoxybenzaldehyde, potassium hydroxide, L-tyrosine, 2,2':6',2"-terpyridine and copper chloride as raw materials, a novel copper-based complex (I) was successfully synthesized in the anhydrous methanol solvent. The crystal structure of (I) was characterized by X-ray single crystal diffraction technique. The results show that (I) is a mononuclear copper complex with five-coordination, and its coordination geometry is a trigonal bipyramidal structure, in which nitrogen atoms and chlorine atoms coordinate with the copper metal center together. The results of the MTT assay show that the inhibitory activity of (I) against the tested cancer cells is significantly higher than its toxicity to non-cancer cells (for example, the $IC_{50}$ value of (I) against MCF-7 cells is 25.53 μM, while the $IC_{50}$ value against human renal tubular epithelial cells HK-2 is 292.78 μM), exhibiting good selective cytotoxicity. Thus, the cytotoxicity activity of (I) provides a valuable insight in terms of the future design of metal-based drugs.

## References

[1] Kaim, W., & Rall, J. (1996). Copper—A "modern" bioelement. *Angewandte Chemie International Edition, 35*(1), 43–60. https://doi.org/10.1002/anie.199600431

[2] Krupa, K., Lesiów, M., Stokowa-Sołtys, K., Starosta, R., Ptaszyńska, N., Łęgowska, A., Rolka, K., Wernecki, M., Cal, M., & Jeżowska-Bojczuk, M. (2018). Copper(II) complexes with *Fusobacterium nucleatum* adhesin FadA: Coordination pattern, physicochemical properties and reactivity. *Journal of Inorganic Biochemistry, 189*, 69–80. https://doi.org/10.1016/j.jinorgbio.2018.09.012

[3] Wu, T., Wang, S., Lv, Y., Fu, T., Jiang, J., Lu, X., Yu, Z., Zhang, J., Wang, L., & Zhou, H. (2022). A new bis(thioether)-dipyrrin N2S2 ligand and its coordination behaviors to nickel, copper and zinc. *Dalton Transactions, 51*(25), 9699–9707. https://doi.org/10.1039/d2dt01282k

[4] Krasnovskaya, O., Naumov, A., Guk, D., Gorelkin, P., Erofeev, A., Beloglazkina, E., & Majouga, A. (2020). Copper coordination compounds as biologically active agents. *International Journal of Molecular Sciences, 21*(11), 3965. https://doi.org/10.3390/ijms21113965

[5] Fan, L., Tian, M., Liu, Y., Deng, Y., Liao, Z., & Xu, J. (2017). Salicylate•phenanthroline copper(II) complex

induces apoptosis in triple-negative breast cancer cells. *Oncotarget, 8*(18), 29823–29832. https://doi.org/10.18632/oncotarget.15961

[6] Fan, R., Wei, J. C., Xu, B. B., Jin, N., Gong, X. Y., & Qin, X. Y. (2023). A novel chiral oxazoline copper(II)-based complex inhibits ovarian cancer growth in vitro and in vivo by regulating VEGF/VEGFR2 downstream signaling pathways and apoptosis factors. *Dalton Transactions, 52*(33), 11427–11440. https://doi.org/10.1039/d3dt01648j

[7] Hou, X. X., Ren, Y. P., Luo, Z. H., Jiang, B. L., Lu, T. T., Huang, F. P., & Qin, X. Y. (2021). Two novel chiral tetranucleate copper-based complexes: Syntheses, crystal structures, inhibition of angiogenesis and the growth of human breast cancer in vitro and in vivo. *Dalton Transactions, 50*(41), 14684–14694. https://doi.org/10.1039/d1dt02033a

[8] Xu, B. B., Jin, N., Liu, J. C., Liao, A. Q., Lin, H. Y., & Qin, X. Y. (2024). Arene-arene coupled disulfamethazines (or sulfadiazine)-phenanthroline-metal(II) complexes were synthesized by in situ reactions and inhibited the growth and development of triple-negative breast cancer through the synergistic effect of antiangiogenesis, anti-inflammation, pro-apoptosis, and cuproptosis. *Journal of Medicinal Chemistry, 67*(9), 7088–7111. https://doi.org/10.1021/acs.jmedchem.3c02432

[9] Liao, A. Q., Wen, J., Wei, J. C., Xu, B. B., Jin, N., Lin, H. Y., & Qin, X. Y. (2024). Syntheses, crystal structures of copper(II)-based complexes of sulfonamide derivatives and their anticancer effects through the synergistic effect of anti-angiogenesis, anti-inflammation, pro-apoptosis and cuproptosis. *European Journal of Medicinal Chemistry, 280*, 116954. https://doi.org/10.1016/j.ejmech.2024.116954

[10] Ziesak, A., Wesp, T., Hübner, O., Kaifer, E., Wadepohl, H., & Himmel, H. J. (2015). Counter-ligand control of the electronic structure in dinuclear copper-tetrakisguanidine complexes. *Dalton Transactions, 44*(44), 19111–19125. https://doi.org/10.1039/c5dt03270a

[11] Tsang, T., Davis, C. I., & Brady, D. C. (2021). Copper biology. *Current Biology, 31*(9), R421–R427. https://doi.org/10.1016/j.cub.2021.03.054

[12] Hussain, A., AlAjmi, M. F., Rehman, M. T., Amir, S., Husain, F. M., Alsalme, A., Siddiqui, M. A., AlKhedhairy, A. A., & Khan, R. A. (2019). Copper(II) complexes as potential anticancer and nonsteroidal anti-inflammatory agents: In vitro and in vivo studies. *Scientific Reports, 9*, 1–17. https://doi.org/10.1038/s41598-019-41063-x

[13] Wilcken, R., Zimmermann, M. O., Lange, A., Joerger, A. C., & Boeckler, F. M. (2013). Principles and applications of halogen bonding in medicinal chemistry and chemical biology. *Journal of Medicinal Chemistry, 56*(4), 1363–1388. https://doi.org/10.1021/jm3012068

[14] Tulchinsky, Y., Hendon, C. H., Lomachenko, K. A., Borfecchia, E., Melot, B. C., Hudson, M. R., Tarver, J. D., Korzyński, M. D., Stubbs, A. W., Kagan, J. J., Lamberti, C., Brown, C. M., & Dincă, M. (2017). Reversible capture and release of $Cl_2$ and $Br_2$ with a redox-active metal-organic framework. *Journal of the American Chemical Society, 139*(16), 5992–5997. https://doi.org/10.1021/jacs.7b02161

[15] Bickerton, L. E., Docker, A., Sterling, A. J., Kuhn, H., Duarte, F., Beer, P. D., & Langton, M. J. (2021). Highly active halogen bonding and chalcogen bonding chloride transporters with non-protonophoric activity. *Chemistry – A European Journal, 27*(45), 11738–11745. https://doi.org/10.1002/chem.202101681

[16] Jentzsch, A. V., & Matile, S. (2015). Anion transport with halogen bonds. *Topics in Current Chemistry, 358*, 205–239. https://doi.org/10.1007/128_2014_541

[17] Wei, Q., Ge, B. D., Zhang, J., Sun, A. H., Li, J. H., Han, S. D., & Wang, G. M. (2019). Tripyridine-derivative-derived semiconducting iodo-argentate/cuprate hybrids with excellent visible-light-induced photocatalytic performance. *Chemistry – An Asian Journal, 14*(2), 269–277. https://doi.org/10.1002/asia.201801555

[18] Kodera, M., Kajita, Y., Tachi, Y., & Kano, K. (2003). Structural modulation of Cu(I) and Cu(II) complexes of sterically hindered tripyridine ligands by the bridgehead alkyl groups. *Inorganic Chemistry, 42*(4), 1193–1203. https://doi.org/10.1021/ic026008m

[19] Dorofeeva, V. N., Pavlishchuk, A. V., Kiskin, M. A., Efimov, N. N., Minin, V. V., Lytvynenko, A. S., Gavrilenko, K. S., Kolotilov, S. V., Novotortsev, V. M., & Eremenko, I. L. (2019). Co(II) complexes with a tripyridine ligand, containing a 2,6-di-tert-butylphenolic fragment: Synthesis, structure, and formation of stable radicals. *ACS Omega, 4*(1), 203–213. https://doi.org/10.1021/acsomega.8b02595

[20] Suntharalingam, K., White, A. J., & Vilar, R. (2009). Synthesis, structural characterization, and quadruplex

DNA binding studies of platinum(II)-terpyridine complexes. *Inorganic Chemistry, 48*(19), 9427–9435. https://doi.org/10.1021/ic901319n

[21] Dolomanov, O. V., Bourhis, L. J., Gildea, R. J., Howard, J. A. K., & Puschmann, H. (2009). OLEX2: A complete structure solution, refinement and analysis program. *Journal of Applied Crystallography, 42*(2), 339–341. https://doi.org/10.1107/S0021889808042726

[22] Sheldrick, G. M. (2015). Crystal structure refinement with SHELXL. *Acta Crystallographica Section C: Structural Chemistry, 71*(1), 3–8. https://doi.org/10.1107/S2053229614024218